CHAPTER VI

Cyclic Voltammetry Study on Zinc and Air Electrodes in Gelled KOH Electrolyte

6.1 Introduction

An immediate consequence of gelling is the decrease in the freely available KOH concentration to the electrodes. Further the elastic jelly granules are likely to contribute in the increase of the interfacial resistance due to the lack of continuous and uniform electrode-gelled electrolyte interface [*Vinod and Vijayamohanan, 2000*]. Thus, the cyclic voltammetry technique was utilized to study the consequence of gelling and the use of hydroponics gel, on the electrode kinetics and make a comparison with the electrode properties in aqueous electrolyte. Cyclic voltammetry analysis was also performed on the electrode coated with thin agar layer in gelled KOH as its application had been demonstrated as beneficial to the zinc-air cell discharge capabilities [*Othman et. al, 2001; Othman et. al, 2002a; Othman et. al, 2002b*].

6.2 Experimental

Experimentation was carried out in a home-made single compartment electrolytic cell of 45-cm^3 volume. The electrolytic cell was modified from the

zinc-air cell plastic casing (refer Figure 3.1). A plastic cap with a 1 cm opening replaced one of the L-shaped plastic rings and a hole was made in the middle of the casing for the reference electrode insertion.

The working electrode was a 0.4-mm thick 99.99% zinc foil or the commercial air electrode, which were cut into a small piece of 12 mm x 12 mm dimension. The zinc electrodes were pretreated in acetone for degreasing, followed by a short immersion in 50 % v/v HCl until a light, matt and clean surface was apparent, and finally rinsed in deionized water [*Wilcox and Mitchell, 1989; Zhu et.al, 1997*]. The electrode was attached to the plastic cap with the 1 cm opening by means of epoxy resin adhesive, so that the apparent exposed area of the working electrode was a circular area of 1 cm in diameter (0.79 cm^2). The schematic diagram of the electrolytic cell and its components is given in Figure 6.1. The electrolyte was a 6-M aqueous KOH solution immobilized with hydroponics gel. The counter electrode was a nickel foil 4.3 cm in diameter (14.5 cm^2). The separation between the electrodes was 2.8 cm. The cyclic voltammetry measurements were conducted using a BAS 100 A Electroanalytical Analyzer. The potentials were recorded versus an Ag/AgCl reference electrode. All measurements were performed at a room temperature of 30°C.

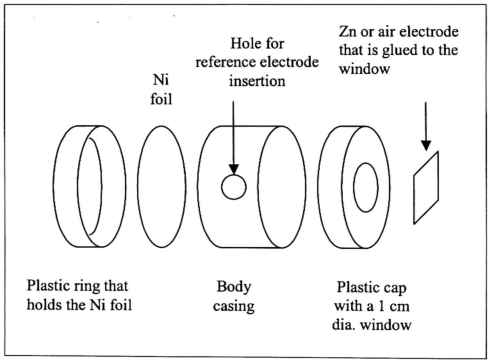

Figure 6.1. Schematic diagram showing the electrolytic cell assembly.

The cyclic voltammetry studies were made in the voltage envelope of –2500 mV to +2000 mV at scanning rates of 10 mV s^{-1} and 25 mV s^{-1}. The electrochemical behaviour of the zinc and air electrodes in alkaline electrolyte were studied in three different electrolyte conditions, viz., (i) in gelled KOH electrolyte, in which the aqueous KOH electrolyte was immobilized using hydroponics gel, (ii) in gelled KOH and the electrode was coated with a thin agar layer, and for comparison (iii) in aqueous KOH. Details regarding the electrolyte gelling and, preparation and application of the agar layer onto the electrode can be found in Sections 3.2.1 and 4.3.2, respectively.

6.3 Results

6.3.1 Zinc electrode

The cyclic voltammogram of zinc in aqueous KOH obtained at 10 mV s^{-1} is shown in Fig. 6.2 together with the notation used for designating the peaks. It shows the typical electrochemical behaviour of zinc in alkaline electrolyte as reported by many workers [*Binder et. al, 1981; Cabot et. al, 1986; Cai and Park, 1996; Rehim et. al, 1995 and Renuka et. al, 2001*]. The anodic span exhibits active and passive regions prior to oxygen evolution potential. Starting at –2000 mV two anodic peaks AI and AII appear at –1054 mV and –966 mV respectively, followed by an abrupt drop in the anodic dissolution current indicating the onset of passivation. The passive region extends to a potential

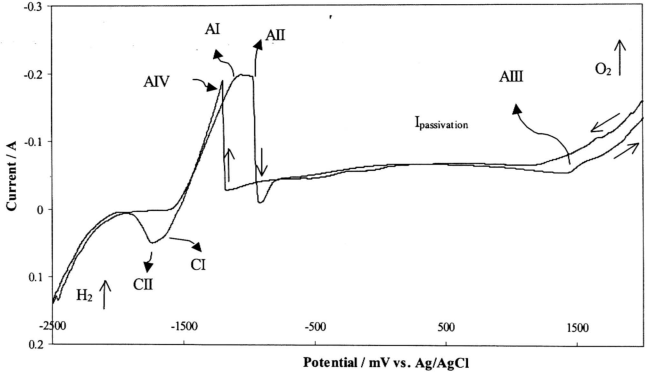

Figure 6.2. Cyclic voltammogram of zinc in 6 M aqueous KOH electrolyte at a scan rate of 10 mV s^{-1} exhibiting the active, passive, transpassive and gas evolution regions.

range of –1480 mV whereby a small hump emerges subsequently prior to the oxygen evolution potential. Possibly this can be attributed to the transpassive anodic peak AIII. Having reached 2000 mV, the sweep was reversed to its starting potential. The reverse sweep exhibits an activation anodic peak AIV at –1200 mV, which lies within the active dissolution range, and two cathodic peaks CI and CII at –1674 mV and –1710 mV respectively, preceding the hydrogen evolution potential.

The anodic peak AI is attributed to the formation of porous and non-protective $Zn(OH)_2$ due to the local supersaturation of tetrahydroxy zincate species $Zn(OH)_4^{2-}$ [*Rehim et. al, 1995*], whereas the anodic peak AII is correlated to the formation of a compact, coherent and highly protective $Zn(OH)_2$ [*Rehim et. al, 1995*]. The occurrence of the transpassive anodic peak AIII is attributed to the transformation of Zn^{2+} in the passive film to a higher oxidation state most probably peroxide ZnO_2 [*Rehim et. al, 1995*],

$$Zn^{2+} + 4OH^- \rightarrow ZnO_2 + 2H_2O + 2e \qquad (6.1)$$

Reversing the potential sweep and upon reaching the passivation potential sufficiently permits enough time in which the alkaline electrolyte dissolves the passive $Zn(OH)_2$ film,

$$Zn(OH)_2 + 2OH^- \rightarrow Zn(OH)_4^{2-} \qquad (6.2)$$

Thus, the metal activated at certain potential, dissolves and forms the tetrahydroxy zincate that leads to the appearance of the anodic peak AIII [*Rehim et. al, 1995*]. Finally the appearance of cathodic peaks CI and CII is associated to the electroreduction of the remaining passive $Zn(OH)_2$ previously formed during the anodic sweep to Zn.

The splitting of the cathodic peak into a doublet indicates that two reduction processes are involved. The more positive peak CI is assigned to the reduction of prepassive species or film [*Cai and Park, 1996*], which is related to the reactions,

$$Zn(OH)_2 + 2e \rightarrow Zn + 2OH^- \qquad E^0 = -1.246V \qquad (6.3)$$

or

$$ZnO + H_2O + 2e \rightarrow Zn + 2OH \qquad E^0 = -1.248V \qquad (6.4)$$

The more negative peak CII is related to the zincate species reaction [*Cai and Park, 1996*],

$$Zn(OH)_4^{2-} + 2e \rightarrow Zn + 4OH^- \qquad E^0 = -1.285V \tag{6.5}$$

Figure 6.3a depicts the cyclic voltammograms of Zn electrode in gelled KOH electrolyte, with one which the Zn electrode was coated with a thin agar layer, in comparison to the cyclic voltammogram in aqueous KOH at scan rate of 10 mV s^{-1}. For clarity of comparison the anodic sweep and the cathodic sweep are separated and presented in Figures 6.3b and 6.3c respectively.

In the anodic sweep, the first consequence of the gelling of the electrolyte is the onset of the zinc dissolution, which shifts positively towards a less negative potential by nearly 100 mV. Another notable feature is that the anodic peaks AI and AII seem to coalesce with each other and appear as one peak, after which this peak will be denoted as anodic peak A only. The value of the anodic peak current and the passivation current are substantially reduced by 40 % and 80 % respectively as a result of gelling. The application of the agar layer onto the zinc electrode does not affect the maximum current of the anodic peak A but shifted the anodic peak A negatively after being drawn out positively. The transpassive anodic peak AIII does not appear for the gelled electrolyte.

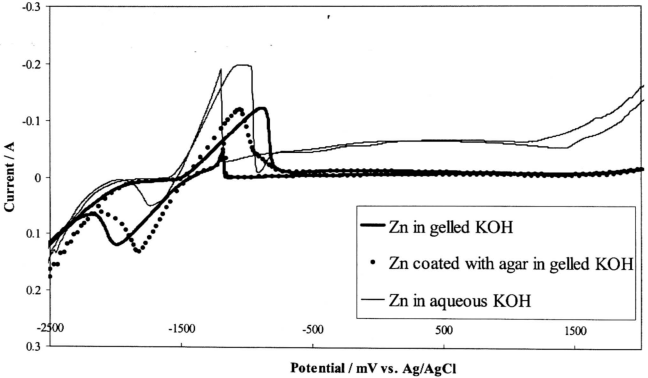

Figure 6.3 (a). The electrochemical behaviour of zinc in gelled KOH electrolyte in comparison to its properties in aqueous KOH electrolyte.

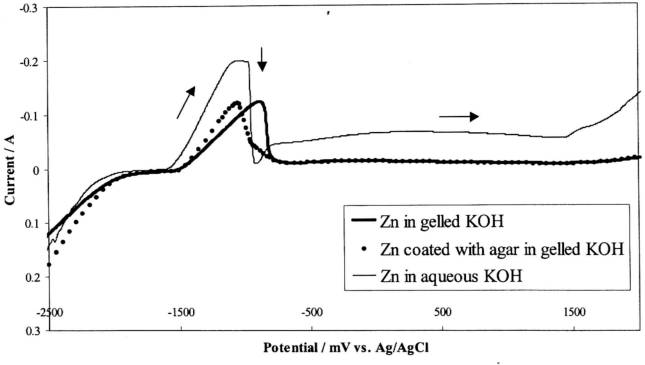

Figure 6.3 (b). Anodic sweep of the cyclic voltammetry of zinc in different conditions.

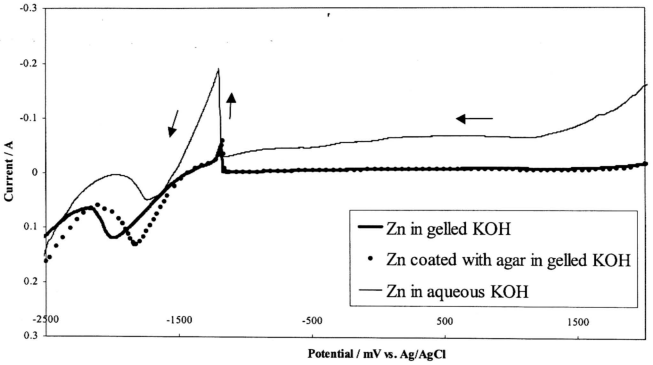

Figure 6.3 (c). Cathodic sweep of the cyclic voltammetry of zinc in different conditions.

In the reverse sweep, the activation anodic peak AIV is significantly suppressed, whereas the cathodic peak is notably enhanced. Note also that the cathodic peaks CI and CII merge into a single peak and thus will be designated as cathodic peak C only. The gelling of the electrolyte causes the cathodic peak C to be shifted to a more negative value. Coating the zinc with agar promotes the cathodic peak towards a positive direction and also increases the peak current slightly.

Another notable consequence of the gelling of the electrolyte is its effect on the oxygen and hydrogen evolution. On the far positive end particularly, the oxygen evolution potential is markedly extended from around +1700 mV to +2000 mV, while in the negative end the hydrogen evolution potential is shifted from –2060 mV to a more negative potential of –2240 mV.

Figure 6.4 depicts the cyclic voltammetry curves of the Zn electrode at higher scanning rates of 25 mV s^{-1}. All the features are similar and the observed changes are typical compared to those obtained at a scan rate of 10 mV s^{-1}. However note that for the curve of zinc in aqueous KOH the peak separation, ΔE_P between the anodic peak A1 and AII increases considerably. Anodic peaks AI and AII now appear at –1140 mV and –532 mV respectively (ΔE_P=608 mV) compared to the values of –1054 mV and –966 mV (ΔE_P=88 mV) registered at scan rate of 10 mV s^{-1} respectively.

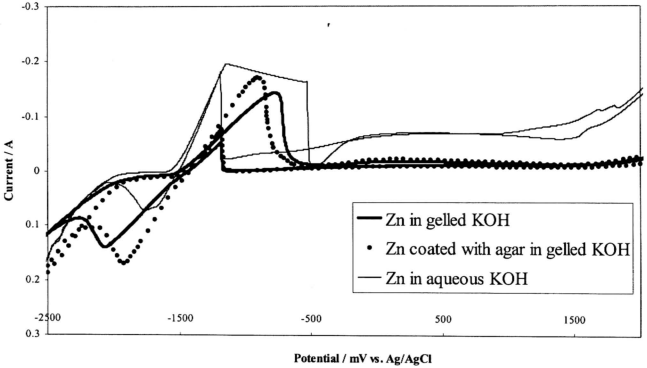

Figure 6.4. Cyclic voltammetry curves of zinc at a higher scan rate of 25 mV s^{-1} in the gelled and aqueous KOH electrolytes.

6.3.2 Air electrode

The results of the cyclic voltammetry measurements of the fibrous carbon-type air electrode, recorded at 10 mV s^{-1}, are shown in Fig 6.5a. The CV pattern of the air electrode in aqueous KOH indicates a well-defined single anodic peak, P and a corresponding cathodic peak, Q prior to the onset of the oxygen evolution. Conversely, the voltammograms of the air electrode in gelled KOH do not reveal any apparent redox peaks. The cathodic cycle of the voltammograms displays excellent reversibility whereas the anodic cycle shows large hysteresis. The cathodic current starts around –300 mV and it increases gradually until –1500 mV, upon which the hydrogen begins to evolve as marked by the rapid current rise. The cathodic current between the potential limits –300 mV and –1500 mV is of particular interest as it may be regarded as resulting from the reduction of oxygen from the ambient air,

$$O_2 + 2H_2O + 4e \rightarrow 4OH^- \qquad (6.6)$$

A closer view of the voltammograms in this potential region, as depicted in Fig. 6.5b, reveals the cyclic voltammetry of that gelled electrolyte shows a slight hysteresis pattern. However, coating the electrode with the agar film apparently diminishes the hysteresis. The gelling of the electrolyte also lowers the cathodic current substantially and the agar coating of the air electrode causes a further drop. The current divergence increases cathodically.

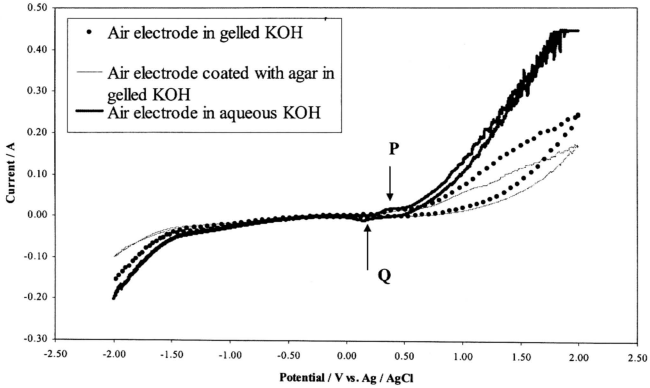

Figure 6.5 (a). Cyclic voltammograms of the air electrode in the gelled and aqueous KOH electrolyte at a scan rate of 10 mV s^{-1}.

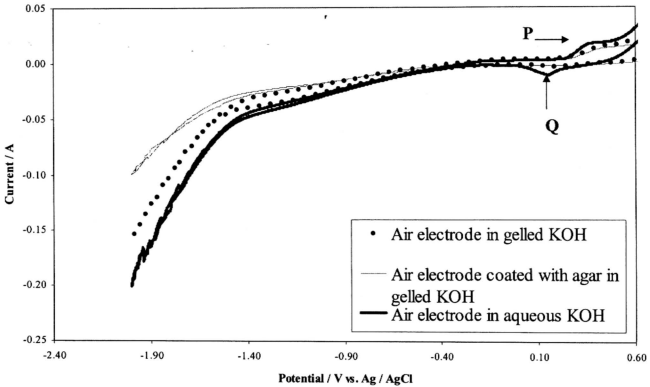

Figure 6.5 (b). A closer view of the cyclic voltammetry curves of the air electrode (at a scan rate of 10 mV s^{-1}) in the cathodic region.

Table 6.1 below lists the current value in the negative sweep registered at three different potentials within the potential limits.

Table 6.1. The cathodic current values between the potential limits –300 mV and –1500 mV indicating the effects of the electrolyte gelling and the agar coating.

Potential (mV)	**Cathodic Current (mA)**		
	Aqueous KOH	**Gelled KOH**	**Gelled KOH with agar coating**
-500	8.0	7.5	5.9
-950	26.2	23.3	16.0
-1400	48.0	39.0	28.3

Figure 6.6 presents the voltammograms at a higher scan rate of 25 mV s^{-1} displaying similar voltammetric patterns and trends. However, the redox couple before the oxygen evolution potential is more pronounced.

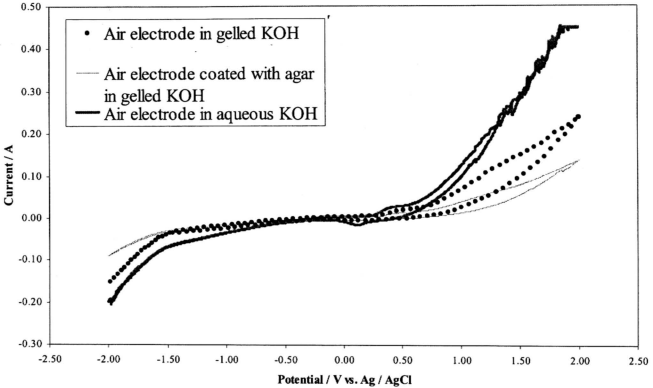

Figure 6.6. Cyclic voltammetry curves of the air electrode at a higher scan rate of 25 mV s^{-1}.

In the anodic cycle, the anodic current due to oxygen generation is observed in the potential region more anodic than +500 mV. The large hysteresis pattern is indicative of the irreversibility of the air electrode, which is a renowned problem in such electrodes. The redox couple centred around +390 mV and –150 mV is attributed to the electrochemical characteristics of nickel in alkaline electrolyte, which originated from the nickel support and current collector of the air electrode.

In concentrated KOH electrolyte, nickel is spontaneously covered with $Ni(OH)_2$ layer [*Guzman et. al, 1978*]. The anodic peak P is associated with the oxidation of hydrated nickel hydroxide $Ni(OH)_2$ to hydrated nickel oxyhydroxides *NiOOH* [*de Souza et. al, 1997; Guzman et. al, 1978*]. The cathodic peak Q is associated with the reduction of *NiOOH* to $Ni(OH)_2$ [*de Souza et. al, 1997; Guzman et. al, 1978*]. The overall redox reaction can be written as [*Barral et. al, 1995; Mo et. al, 1996*],

$$Ni(OH)_2(hyd.) + OH^- \rightarrow NiOOH(hyd.) + H_2O + e \qquad (6.7)$$

A similar voltammogram on the air electrode exhibiting an anodic and cathodic peak preceding the oxygen evolution was also observed by others [*Matsumoto et. al, 1977; Tiwari et. al, 1995; Tiwari et. al, 1996; Vermeiren et. al, 1987*], which were also ascribed to the Ni(II)/Ni(III) redox couple.

6.4 Discussion

The gelled KOH electrolyte was in the form of loosely bound elastic jelly granules. Therefore, the immediate consequence of gelling is the decrease in the freely available KOH concentration to the zinc electrode. Another notable feature of diffusion transport in gels is the existence of simultaneously competitive diffusion and retention processes [*Lakatos and Lakatos-Szabo, 1998*]. These characteristics of the gelled electrolyte substantially affect the electrode kinetics.

6.4.1 Zinc electrode

The cyclic voltammograms of zinc revealed that the gelling of the aqueous KOH electrolyte causes a considerable increase in the onset of zinc electrode dissolution. Furthermore, the anodic peak A is shifted towards the positive direction and the cathodic peak C is shifted towards the negative direction. These trends are most likely attributed to the considerable increase in the interfacial ohmic resistance and the electrolyte diffusion transport impedance in the gelled electrolyte, as verified by *Vinod and Vijayamohanan (2000)*, using the impedance spectroscopy technique on a maintenance-free lead acid battery. As expected the zinc electrode passivation accelerated as a result in the decrease in the freely available KOH electrolyte that is entrapped in the elastic jelly granules. In aqueous electrolyte the anodic current peak was at 197.5 mA while

in the gelled electrolyte the current peak was at 122.1 mA prior to the onset of passivation respectively. The fact that the passivation occurs at a much lower peak current suggests that the passivation is substantially accelerated in gelled electrolyte.

Another significant consequence due to the lack in the free electrolyte is that the activation anodic peak AIII is appreciably suppressed. The anodic peak AIII is often associated with the problems encountered in the development of rechargeable alkaline zinc batteries. Dissolution of the passive discharge product of $Zn(OH)_2$ or ZnO causes problems of capacity loss, short life-time and dendrite formation in secondary alkaline zinc batteries [*McLarnon and Cairns, 1991*]. The limited free electrolyte is easily saturated with zincate ions and thus minimizes the dissolution of the precipitated discharge product. It is believed that the gelled KOH also effectively reduces the migration of the soluble zincate ions and traps them within the gel structure. A further manifestation of the suppression of the dissolution of the discharge product is the substantial decrease in the passivation current, I_{pass} as a result of gelling. The passivating current is related to the chemical dissolution of the passive discharge product [*Prentice et. al, 1991 and Rehim et. al, 1995*]. As a result, the suppression of the passive film dissolution also promotes the redeposition of zinc, as is evident from the features of the cathodic peak C. Both the intensity and the area under the curve of the cathodic peak C are notably enhanced in gelled electrolyte. It is well known that in order to reduce the problems of shape change and capacity fading on repeated

cycling of the zinc anode, the dissolution and migration of the discharge product must be controlled. From this point of view, the use of gelled electrolyte shows potential prospects.

Apart form affecting the features of the anodic and cathodic peaks, the gelling of the electrolyte also attenuates both the oxygen and hydrogen evolution reactions. These beneficial effects are particularly useful in the development of rechargeable alkaline zinc batteries. In aqueous based electrolyte batteries, the charging process causes considerable water loss due to the decomposition of the water. By extending the oxygen evolution potential sufficiently high towards the positive end, the electrolyte water loss can thus be minimized. The increase in the hydrogen overvoltage on zinc in an alkaline medium is another added advantage, especially without the inclusion of any additives. The losses due to wasteful corrosion could be minimized. These beneficial effects on the use of gelled aqueous based electrolyte have in fact been observed in the maintenance-free lead acid battery [*Vinod and Vijayamohanan, 1994; Vinod et. al, 1998*]. However the authors did not attempt to explain these phenomena. The increase in the hydrogen overvoltage in gelled electrolyte is most possibly attributed to the decrease in the activity of water [*Dirkse and Timmer, 1969*] and the suppression of the zinc dissolution [*Ruetschi, 1967*], which are due to the limited free electrolyte medium. The suppression of zinc dissolution in gelled electrolyte is clearly evident from the cyclic voltammogram. The onset of zinc dissolution is shifted anodically by nearly 100 mV.

The cyclic voltammogram of zinc coated with agar in gelled KOH lies in between that of zinc in aqueous KOH and zinc in gelled KOH. The purpose of the agar layer is to improve the electrode-gelled electrolyte interface and also to preserve the electrode wettability. As anticipated, the application of a thin agar layer improves the zinc electrode kinetics in gelled KOH; the anodic peak A is shifted negatively after being drawn out positively, and the cathodic peak C is decreased towards a less negative value after being shifted negatively. These trends support our presumption on the role of agar between the electrode-gelled electrolyte interface [*Othman et. al, 2001; Othman et. al, 2002a; Othman et. al, 2002b*].

6.4.2 Air electrode

The oxygen reduction reaction from the ambient air occurred in the potential range of –300 mV to –1500 mV as it appeared in the cyclic voltammetry analysis of the air electrode. As anticipated, the electrolyte gelling reduces the cathodic current substantially, as in the case of the zinc electrode. Apart from the hindrances caused by the interfacial resistance between the electrode-gelled electrolyte and the diffusion transport impedance in a gel structure, another contributing factor is the design of the air electrode itself. The commercial air electrode used in this work consists of a laminated structure of fibrous carbon sandwiched against a nickel mesh support and current collector. Its schematic cross-sectional diagram is given below.

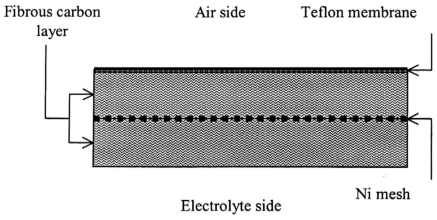

Figure 6.7. Schematic cross-sectional diagram of the air electrode.

The airside of the electrode is coated with a semi-permeable Teflon membrane. The fibrous carbon is also dispersed with a manganese oxide catalyst and PTFE binder. Its design has been customized for optimum performance for use in a fuel cell using liquid electrolyte. Thus the use of a gelled electrolyte in the form of loosely bound elastic jelly granules would most likely affect the air electrode performance. The jelly granules could not penetrate the fibrous carbon layer, hence only the outer side was utilized. This may explain the absence of the voltammetric peaks prior to the oxygen evolution potential in the voltammetric sweeps of the air electrode in gelled electrolyte. This indicates that the electrolyte penetration did not even reach the nickel screen of the electrode or that its concentration at this site was too small to indicate any significant peak.

The application of agar film onto the air electrode did not improve the cathodic current profiles. The oxygen reduction process is relatively slow, complex and involves a rate-limiting stage, which relates to the formation of hydroperoxide ions HO_2^- [*Bender et. al, 1995; Vincent et. al, 1984*]. Inserting an additional agar film between the electrode-gelled interface might have probably further hindered the reduction process. Thus how could the application of agar film onto the air electrode beneficially improve the zinc-air cells discharge capacities as observed in the previous studies ? [*Othman et. al, 2001; Othman et. al, 2002a; Othman et. al, 2002b*]. Zinc-air cells are susceptible to water loss and hence the electrolyte drying out due to the permeability of the air electrode. Therefore, the air electrode-gelled electrolyte interface is mainly affected. Furthermore, during cell discharge heat is generated and this might accelerate the process. Accordingly, coating the electrode with an agar film would keep the interface necessarily wet throughout the cell discharge and as a result improve the cell discharge capacity.

6.5 Summary

The cyclic voltammetry technique has been used to establish the influence of the electrolyte gelling on the zinc and air electrodes kinetics in an alkaline electrolyte. The immobilization of the electrolyte causes considerable hindrance to the electrode kinetics, which is mainly due to the increase in the interfacial resistance and diffusion transport impedance. Other than these, the use of

hydroponics gel did not result in any adverse effects. The application of the agar layer as an electrolyte reservoir between the electrode-gelled electrolyte interface seems to ease the hindrance. For the zinc electrode, the gelling of the electrolyte possesses some advantages. The limited free electrolyte nature of the gelled electrolyte effectively minimizes the passive film dissolution, improves zinc redeposition and suppresses both oxygen and hydrogen gassing potentials. These beneficial effects of gelling are of particular interest in the development of rechargeable alkaline zinc batteries. The design of the commercial air electrode utilized in this work might not be suitable for use with gelled electrolyte as the fibrous carbon structure limits the gelled electrolyte penetration. The application of agar coating on the zinc electrode seemed to ease the interfacial hindrance, however, for the air electrode it did not improve the cathodic current profile. Nevertheless it is still essential in maintaining the wettability of the electrode and has proven beneficial to zinc-air discharge performance.

References

Barral, G., Njanjo-Eyoke, F. and Maximovitch, S., "Growth of a nickel oxide layer on a rotating nickel electrode in a non-buffered solution of sodium sulfate", Electrochim. Acta 40 (**1995**) 709-718

Bender, S.F., Cretzmeyer, J.W. and Reise, T.F., "Zinc-air cells", in: Handbook of Batteries, Linden, D., (Editor), McGraw-Hill Inc., 2nd Ed. (**1995**) pg. 13.1-13.20

Binder, L., Odar, W. and Kordesh, K., "A study of rechargeable zinc electrodes for alkaline cells requiring anodic limitation", J. Power Sources 6 (**1981**) 271-289

Cabot, P.L., Cortes, M., Centellas, F.A., Garrido, J.A. and Perez, E., "Potentiodynamic passivation of zinc in aqueous KOH solutions", J. Electroanal. Chem. 201 (**1986**) 85-100

Cai, M. and Park, S-M., "Spectroelectrochemical studies on dissolution and passivation of zinc electrodes in alkaline solutions", J. Electrochem. Soc. 143 (**1996**) 2125-2131

de Souza, L.M.M., Kong, F.P., McLarnon, F.R. and Muller, R.H., "Spectroscopic ellipsometry study of nickel oxidation in alkaline solution", Electrochim. Acta 42 (**1997**) 1253-1267

Dirkse, T.P. and Timmer, R., "The corrosion of zinc in KOH solutions", J. Electrochem. Soc. 116 (**1969**) 162-165

Guzman, R.S.S., Vilche, J.R. and Arvia, A.J., "Rate processes related to the hydrated nickel hydroxide electrode in alkaline solutions", J. Electrochem. Soc. 125 (**1978**) 1578-1587

Lakatos, I. and Lakatos-Szabo, J., "Diffusion of chromium ions in polymer/silicate gels", Colloids and Surfaces A 141 (**1998**) 425-434

Matsumoto, Y., Yoneyama, H. and Tamura, H., "Electrochemical properties of lanthanum nickel oxide", J. Electroanal. Chem. 80 (**1977**) 115-121

McLarnon, F.R. and Cairns, E.J., "The secondary alkaline zinc electrode", J. Electrochem. Soc. 138 (**1991**) 645-663

Mo, Y., Hwang, E. and Scherson, A., "In situ quartz microbalance studies of nickel hydrous oxide films in alkaline electrolytes", J. Electrochem. Soc. 143 (**1996**) 37-43

Othman, R., Yahaya, A.H. and Arof, A.K., "Zinc-air cell with KOH-treated agar layer between electrode and electrolyte containing hydroponics gel", in: New Materials for Electrochemical Systems IV, Savadogo, O. (Editor), Extended Abstract of the 4th International Symposium on New Materials for Electrochemical Systems, 9-13 July, 2001, Montreal, Quebec, Canada, Ecole Polytechnique de Montreal (**2001**) pg. 300-303

Othman, R., Yahaya, A.H. and Arof, A.K., "Zinc-air cell with KOH-treated agar layer between electrode and electrolyte containing hydroponics gel", J. New Mat. Electrochem. Systems 5 (**2002a**) 177-182

Othman, R., Yahaya, A.H. and Arof, A.K., "Zinc-air cell employing porous zinc electrode fabricated from zinc-graphite-natural biodegradable polymer paste",

J. Appl. Electrochem. 32 (**2002b**) 1347-1353

Prentice, G., Chang, Y-C. and Shan, X., "A model for the passivation of the zinc electrode in alkaline electrolyte", J. Electrochem. Soc. 138 (**1991**) 890-894

Rehim, S.S.A., Wahab, S.M.A., Fouad, E.E. and Hassan, H.H., "Passivity and passivity breakdown of zinc anode in alkaline medium", Mater. Corr. 46 (**1995**) 633-638

Renuka, R., Srinivasan, L., Ramamurthy, S., Veluchamy, A. and Venkatakrishnan, N., "Cyclic voltammetry study of zinc and zinc oxide electrodes in 5.3 M KOH", J. Appl. Electrochem. 31 (**2001**) 655-661

Ruetschi, P., "Solubility and Diffusion of hydrogen in strong electrolytes and the generation and consumption of hydrogen in sealed primary batteries", J. Electrochem. Soc. 114 (**1967**) 301-305

Tiwari, S.K., Chartier, P. and Singh, R.N., "Preparation of perovskite-type oxides of cobalt by the malic acid aided process and their electrocatalytic surface properties in relation to oxygen evolution", J. Electrochem. Soc. 142 (**1995**) 148-153

Tiwari, S.K., Singh, S.P. and Singh, R.N., "Effects of Ni, Fe, Cu and Cr substitutions for Co in $La_{0.8}Sr_{0.2}CoO_3$ on electrocatalytic properties for oxygen evolution", J. Electrochem. Soc. 143 (**1996**) 1505-1510

Vermiren, P.H., Leysen, R. King, H.W., Murphy, G.J. and Vandenborre, H., "Oxygen evolution on $La_{0.8}Sr_{0.2}Ni_{0.2}Co_{0.8}O_3$ electrocatalysts in alkaline medium", Int. J. Hydrogen Energy 12 (**1983**) 469-472

Vincent, C.A., Bonino, F., Lazzari, M. and Scrosati, B., in: Modern Batteries. An Introduction to Electrochemical Power Sources, Edward Arnold (Pub.) Ltd. (**1984**) pg. 90

Vinod, M.P. and Vijayamohanan, K., "Effect of gelling on the open circuit potential against time transients of $Pb/PbSO_4$ electrodes at various states of charge", J. Appl. Electrrochem. 24 (**1994**) 44-51

Vinod, M.P. and Vijayamohanan, K., "Effect of gelling on the impedance parameters of $Pb/PbSO_4$ electrode in maintenance-free lead acid batteries", J. Power Sources 89 (**2000**) 88-92

Vinod, M.P., Vijayamohanan, K. and Joshi, S., "Effect of silicate and phosphate additives on the kinetics of the oxygen evolution in valve-regulated lead/acid batteries", J. Power Sources 70 (**1998**) 103-105

Wilcox, G.D. and Mitchell, P.J., "Electrolyte additives for zinc-anoded secondary cells I. Brighteners, levellers and complexants", J. Power Sources 28 (**1989**) 345-359

Zhu, J-L., Zhou, Y-H. and Yang, H., "Effects of lanthanum and neodymium hydroxides on secondary alkaline zinc electrode", J. Power Sources 69 (**1997**) 169-173